SIMULTANEOUS BIAS CORRECTION AND IMAGE SEGMENTATION VIA L_0 REGULARIZED MUMFORD-SHAH MODEL*

Yuping Duan[1] *, Huibin Chang*[2†] *,Weimin Huang*[1]*, Jiayin Zhou*[1]

[1] Institute for Infocomm Research, [2] Tianjin Normal University

ABSTRACT

This paper presents a novel discrete Mumford-Shah model for the simultaneous bias correction and image segmentation(SBCIS) for images with intensity inhomogeneity. The model is based on the assumption that an image can be approximated by a product of true intensities and a bias field. Unlike the existing methods, where the true intensities are represented as a linear combination of characteristic functions of segmentation regions, we employ L_0 gradient minimization to enforce a piecewise constant solution. We introduce a new neighbor term into the Mumford-Shah model to allow the true intensity of a pixel to be influenced by its immediate neighborhood. A two-stage segmentation method is applied to the proposed Mumford-Shah model. In the first stage, both the true intensities and bias field are obtained while the segmentation is done using the K-means clustering method in the second stage. Comparisons with the two-stage Mumford-Shah model show the advantages of our method in its ability in segmenting images with intensity inhomogeneity.

Index Terms— Mumford-Shah model, segmentation, intensity inhomogeneity, L_0 minimization

1. INTRODUCTION

As a fundamental topic in image processing, the goal of image segmentation is to decompose the image domain into local regions. Such techniques are critical in computer aided diagnosis and computer aided treatment. For example, accurate segmentation of coronary arteries is important to quantify coronary artery stenosis.

Mumford and Shah [1] treated the given image as a function and pursued its piecewise smooth approximation, in which the boundaries are referred to the transition between adjacent patches of the approximation. Let $\Omega \in \mathbb{R}^2$ be open and bounded and Γ be a closed subset in Ω. Given an observed image $f : \Omega \to \mathbb{R}$, to find its piecewise smooth approximation u, Mumford and Shah proposed to minimize the following functional:

$$\min_{u,\Gamma} \int_\Omega (f-u)^2 dx + \mu \int_{\Omega\setminus\Gamma} |\nabla u|^2 dx + \lambda |\Gamma|, \qquad (1)$$

where μ and λ are positive parameters and $|\Gamma|$ denotes the length of Γ. Since the Mumford-Shah functional Eq. (1) is non-convex, finding the minimizer is not straightforward and may trap in local minima.

Recently, a two-stage Mumford-Shah(TSMS) model was proposed [2]. It separates the segmentation task of minimizing the functional Eq. (1) into two stages, i.e., the first stage of finding a smooth solution to a convex variant of the Mumford-Shah functional and the second stage of thresholding the solution into different phases for segmentation. More specifically, the convex Mumford-Shah model was proposed as follows

$$\min_u \int_\Omega (f-u)^2 dx + \mu \int_\Omega |\nabla u|^2 dx + \lambda \int_\Omega |\nabla u| dx. \qquad (2)$$

With the solution u solved in the first stage by (2), the segmentation results are obtained by thresholding u with proper threshold(s). Generally speaking, there are the following good characteristics of this two-stage segmentation framework

① The convex variant Mumford-Shah functional in the first stage has the global minimizer u, which can be easily and quickly computed by standard optimization techniques, such as the split-Bregman algorithm [3] and the Chambolle's dual method [4];

② The thresholding in the second phase is done by either K-means method or user specified threshold(s), which can be solved quickly;

③ Neither need to 1) specify the number of segments K ($K \geq 2$) in the first stage nor to 2) recompute u if the thresholds are changed to reveal different segmentation features.

Intensity inhomogeneity (i.e, bias field) occurs in many medical images from different modalities, such as x-ray radiography, computer tomography(CT) and magnetic resonance(MR) images, presenting a considerable challenge in image segmentation. The same phenomenon, caused by nonuniform illumination, also exists in natural images. Several methods have been proposed to deal with the intensity inhomogeneity. Expectation-maximization(EM) and fuzzy c-means(FCM) have been widely employed in these methods [5, 6]. The bias corrected fuzzy c-means(BCFCM) [7] is one of the most successful methods in removing the effect of bias field. It introduces a neighborhood term that enables the class membership of a pixel to be influenced by its neighbors

*THE WORK IS PARTIALLY SUPPORTED BY A*STAR BEP GRANT 132 148 0008,SINGAPORE.

†Dr. Chang Huibin is supported by PHD Programme 52XB1304 of Tianjin Normal University.

to enforce the solution towards a piecewise homogeneous labeling.

In this paper, we propose a novel variant Mumford-Shah model implemented in the two-stage segmentation framework for the tasks of bias correction and image segmentation. Besides the similar merits of the TSMS model, our model has also the following new features

① We model the image as the product of true intensities and a smooth function in the two-stage segmentation framework. Unlike other existing works [8, 9, 10, 11], which are constructed based on the assumption that true intensities are represented as a linear combination of K characteristic functions, each identifying one segmentation region, with K specified at the beginning, our image model does not rely on such assumption;

② We enforce the true intensities to be piecewise constant by making use of L_0 gradient minimization, which minimize the non-zero gradients to approximate prominent structure;

③ To eliminate the effect of bias field, we introduce a neighbor term acting as a regularizer to bias the true intensities towards homogeneity.

For the test image with serious intensity inhomogeneity, both the TSMS model and bias-corrected fuzzy c-means obtain erroneous results with some part incorrectly identified, while our method can provide a very good result, see Fig. 1.

(a) Input (b) TSMS (c) BCFCM (d) Our result

Fig. 1. A three-phase segmentation example.

2. PROBLEM FORMULATION

2.1. Image model

The observed image is modeled as a product of the true intensities generated by the underlying structure and a spatially varying factor called the bias field. Using the logarithmic transformation to the intensities, it allows the artifact to be modeled as an additive bias field

$$f(x) = u(x) + w(x), \quad x \in \Omega, \tag{3}$$

where u and f are the true and observed log-transformed intensities, respectively, and w is the bias field.

2.2. L_0 regularization

In order to regularize the piecewise constant field u, we explore the L_0 gradient minimization to enhance highest-contrast edges by confining the number of non-zero gradients [12]. We denote the gradient $\nabla u_p = (\partial_x u_p, \partial_y u_p)^T$ for each pixel p, which is calculated as the difference between neighboring pixels along x and y directions. The corresponding L_0 measure is expressed as

$$C(u) = \#\{p \mid |\partial_x u_p| + |\partial_y u_p| \neq 0\}, \tag{4}$$

where $\#\{\}$ is the counting operator, outputting the number of p that satisfies $|\partial_x u_p| + |\partial_y u_p| \neq 0$.

2.3. The variant Mumford-Shah model

Based on the image model Eq. (3) and L_0 regularization of the piecewise constant function u, we obtain a new variant of the Mumford-Shah model Eq. (1) in the discrete form

$$\min_{u,w} \Big\{ \sum_p (f_p - u_p - w_p)^2 + \mu \sum_p |\nabla w_p|^2 + \lambda C(u) \Big\}.$$

Similar to BCFCM, we introduce a term that allows the solution of u to be influenced by its neighborhood. We define the modified objective functional E as follows

$$E(u,w) = \sum_p (f_p - u_p - w_p)^2 + \mu \sum_p |\nabla w_p|^2 + \lambda C(u) + \frac{\alpha}{N_R} \sum_p \Big(\sum_{r \in \mathcal{N}_p} (f_r - w_r - u_p)^2 \Big), \tag{5}$$

where α is a positive parameter, $\mathcal{N}_p$ is the set of neighbors in a window around p and $\mathcal{N}_R$ is the cardinality of $\mathcal{N}_p$.

3. MINIMIZATION ALGORITHM

We introduce auxiliary variables h_p and v_p, corresponding to $\partial_x u_p$ and $\partial_y u_p$, respectively, and rewrite the functional E in the following way

$$E(u,w,h,v) = \sum_p (f_p - u_p - w_p)^2 + \mu \sum_p |\nabla w_p|^2 + \lambda C(h,v) + \frac{\alpha}{N_R} \sum_p \Big(\sum_{r \in \mathcal{N}_p} (f_r - w_r - u_p)^2 \Big) + \beta \big((\partial_x u_p - h_p)^2 + (\partial_y u_p - v_p)^2 \big), \tag{6}$$

where $C(h,v) = \#\{p | |h_p| + |v_p| \neq 0\}$ and β is an automatically adapting parameter to control the similarity between variables (h,v) and their corresponding gradients.

The minimization problem (6) is separated into three subproblems w.r.t. u, w and (h,v) as follows

① u-sub problem: for given w and (h,v)

$$\min_u \sum_p (f_p - u_p - w_p)^2 + \frac{\alpha}{N_R} \sum_p \Big(\sum_{r \in \mathcal{N}_p} (f_r - w_r - u_p)^2 \Big) + \beta \big((\partial_x u_p - h_p)^2 + (\partial_y u_p - v_p)^2 \big) \tag{7}$$

② w-sub problem: for given u and (h,v)

$$\min_w \sum_p (f_p - u_p - w_p)^2 + \mu \sum_p |\nabla w_p|^2 + \frac{\alpha}{N_R} \sum_{k \in \mathcal{N}_p} \big((f_p - w_p - u_k)^2 \big) \tag{8}$$

③ (h,v)-sub problem: for given u and w

$$\min_{h,v} \sum_p \big((\partial_x u_p - h_p)^2 + (\partial_y u_p - v_p)^2 \big) + \frac{\lambda}{\beta} C(h,v) \tag{9}$$

3.1. Subproblem 1: computing u

The Euler-Lagrange equation of u-sub problem Eq. (7) gives

us a quadratic function. Similar to [12], we use the Fast Fourier Transform(FFT) to compute the solution of u as follows

$$u = \mathcal{F}^{-1}\Big(\frac{\mathcal{F}(P) + \beta(\mathcal{F}(\partial_x)^*\mathcal{F}(h) + \mathcal{F}(\partial_y)^*\mathcal{F}(v))}{1 + \alpha + \beta(\mathcal{F}(\partial_x)^*\mathcal{F}(\partial_x) + \mathcal{F}(\partial_y)^*\mathcal{F}(\partial_y))}\Big), \quad (10)$$

where $P_p = f_p - w_p + \frac{\alpha}{N_R}\sum_{r\in\mathcal{N}_p}(f_r - w_r)$ for each single term w.r.t. pixel p.

3.2. Subproblem 2: computing w

The optimal condition of w-sub problem Eq. (8) is obtained by pursuing its Euler-Lagrange equation, which is given as follows

$$(1 + \alpha - \mu\Delta)w_p = (1 + \alpha)f_p - \Big(u_p + \frac{\alpha}{N_R}\sum_{r\in\mathcal{N}_p} u_r\Big), \quad (11)$$

where Δ is the Laplace operator. Similarly, the quadratic function Eq. (11) can be solved efficiently by the FFT, i.e.,

$$w = \mathcal{F}^{-1}\Big(\frac{\mathcal{F}(Q)}{1 + \alpha + \mu\mathcal{F}(\Delta)}\Big), \quad (12)$$

where $Q_p = (1+\alpha)f_p - u_p - \frac{\alpha}{N_R}\sum_{r\in\mathcal{N}_p} u_r$ for each single term w.r.t. pixel p.

3.3. Subproblem 3: computing (h, v)

The subproblem Eq. (9) is firstly rewritten as

$$\sum_p \min_{h_p, v_p}\{(h_p - \partial_x u_p)^2 + (v_p - \partial_y u_p)^2 + \frac{\lambda}{\beta}H(|h_p| + |v_p|)\},$$

where $H(|h_p| + |v_p|)$ is a binary function returning 1 if $|h_p| + |v_p| \neq 0$ and 0 otherwise. Each single pixel $p$reaches its minimum under the condition

$$(h_p, v_p) = \begin{cases} (0,0) & (\partial_x u_p)^2 + (\partial_y u_p)^2 \leq \frac{\lambda}{\beta}, \\ (\partial_x u_p, \partial_y u_p) & \text{otherwise.} \end{cases} \quad (13)$$

3.4. Algorithm

We present the alternative algorithm for the proposed model Eq. (5) in Algorithm 1. In numerical implementations, the β_0 and β_{max} are fixed values 2λ and $1E10$, respectively. The γ is set to 1.01, which is tunable to the increase of the β.

Algorithm 1 L_0 Regularized Mumford-Shah Model

Input: image f, parameters μ, λ, β_0, β_{max} and rate γ
Initialization: $w \leftarrow f$, $h \leftarrow \partial_x u$, $v \leftarrow \partial_y u$, $\beta \leftarrow \beta_0$, $i \leftarrow 0$
repeat

- With $w^{(i)}$ and $h^{(i)}$, $v^{(i)}$, solve for $u^{(i)}$ in Eq. (10);
- With $u^{(i)}$, solve for $w^{(i)}$ in Eq. (12);
- With $u^{(i)}$, solve for $h_p^{(i)}$ and $v_p^{(i)}$ in Eq. (13);
- $\beta \leftarrow \gamma\beta$; $i \leftarrow i + 1$.

until $\beta \geq \beta_{max}$
Output: Specify K and implement the K-means method to $u^{(i)}$.

4. NUMERICAL EXPERIMENTS

In this section, we compare the SBCIS model with the TSMS model in order to demonstrate the advantages of the SBCIS model in dealing with intensity inhomogeneity.

4.1. Two-phase segmentation

Example 1: Synthetic images. Fig. 2(a) are two test images seriously affected by intensity inhomogeneity due to nonuniform illumination. As shown in Fig. 2(d), the proposed algorithm performs very well in handling the inhomogeneity while some part of the foreground from the TSMS model is incorrectly identified as the background as shown in Fig. 2(e).

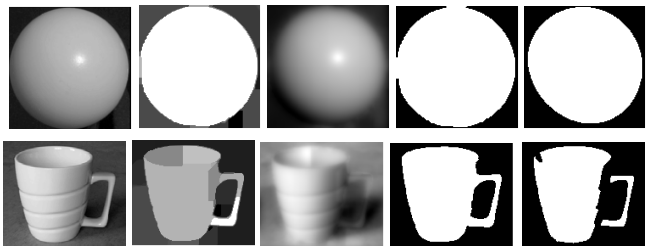

(a) Input (b) u (c) w (d) Our result (e) TSMS

Fig. 2. Applications to natural images.

Example 2: Natural images with noise. Two widely used natural images with intensity inhomogeneity are tested. We add Gaussian zero mean noise with the standard deviation 20 to the test image "rice" and "coins" in Fig. 3(a) to verify the performance of the proposed model in removing noises. Compared to the results of the TSMS model, our model can identify the complete boundaries of the objects contained in test images.

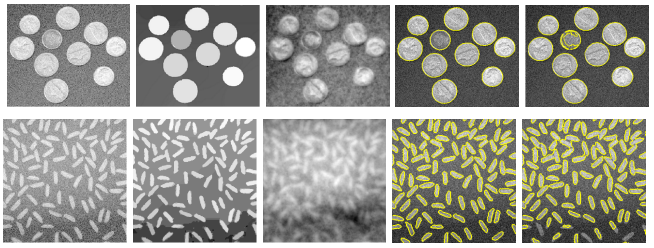

(a) Input (b) u (c) w (d) Our result (e) TSMS

Fig. 3. Applications to noisy images.

Example 3: Vessel images. For vessel images in Fig. 4(a) obtained from [13], the intensity inhomogeneity is obvious as some parts of the vessel boundaries are quite weak. By successfully eliminating the effect of bias field, our model can correctly identify the vessels, while the TSMS model fails to do so. Besides, it is shown in Fig. 4(c) that the estimated bias fields keep smooth in the image domain.

4.2. Multi-phase segmentation

Example 4: CT angiography images. We apply the methods to 2D maximum intensity projection (MIP) images of a real 3D CT angiography data shown in Fig. 5(a). We implemented three-phase segmentation models to extract the vascular

structures from the given MIP images. The segmentation results of the vessel phase (phase 1) containing the aorta and a branch of coronary artery from the proposed model and TSMS model are displayed in Fig. 5(d) and Fig. 5(e), respectively. It is shown that our model can identify the vascular structures from the background accurately.

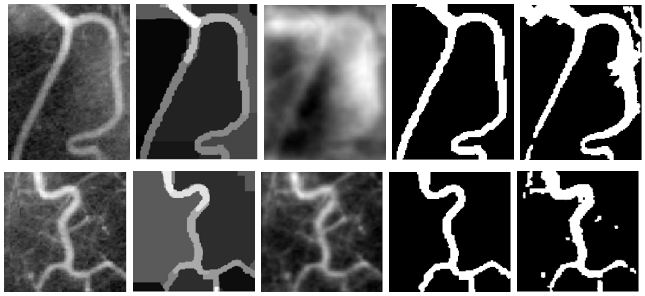

(a) Input (b) u (c) w (d) Our result (e) TSMS

Fig. 4. Applications to real blood vessel images.

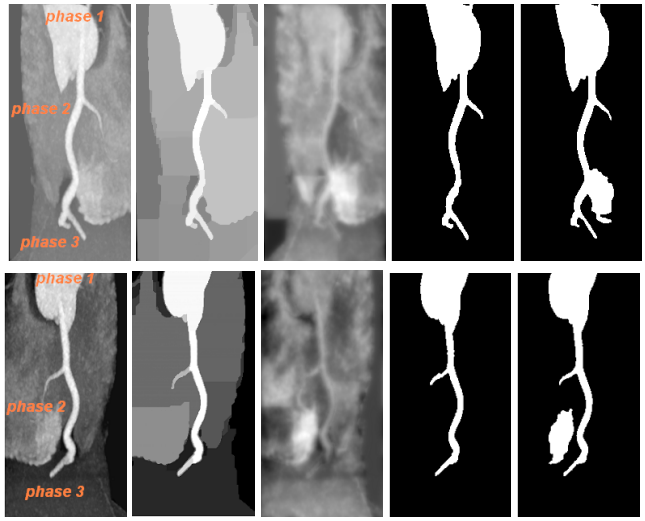

(a) Input (b) u (c) w (d) Our result (e) TSMS

Fig. 5. Applications to CT angiography MIP images.

Example 5: Brain MR images. The original test MR image acquired from a 3T scanner is shown in Fig. 6(a), where the inhomogeneity can be clear seen. In the bias corrected image shown in Fig. 6(b), the intensities within each tissue become quite homogeneous. The segmented results are shown in each phase in Fig. 6(c), (d) and (e), respectively.

To quantitatively evaluate and compare the proposed method and the TSMS model, we use the synthetic MR images with ground truth from BrainWeb: http://www.bic.mni.mcgill.ca/brainweb/. Both 7% of noise and 20% of intensity non-uniformity (INU) are added to the test image. Besides, we added a productive bias field to the test image to enhance the intensity inhomogeneity as shown in Fig. 7(a). The segmentation results of the proposed method and TSMS model are given in Fig.7. The performance precision and sensitivity for our model and the TSMS model are listed in Table 1. It can be seen that both precision and sensitivity of the proposed method are higher than the TSMS model.

(a) Input (b) $f - w$ (c) Phase 1 (d) Phase 2 (e) Phase 3

Fig. 6. Applications of our method to a 3T MR image.

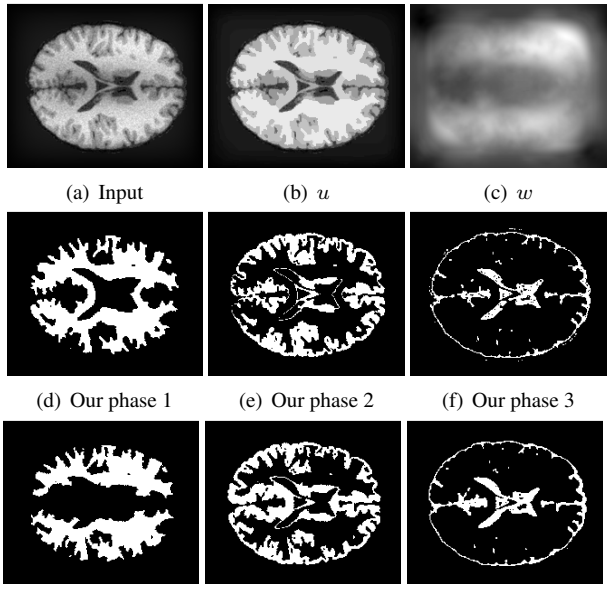

(a) Input (b) u (c) w

(d) Our phase 1 (e) Our phase 2 (f) Our phase 3

(g) TSMS phase 1 (h) TSMS phase 2 (i) TSMS phase 3

Fig. 7. Segmentation results for a synthetic MR image.

Table 1. Precision (P%) and sensitivity (S%) of brain MR image.

	Phase 1		Phase 2		Phase 3	
	P%	S%	P%	S%	P%	S%
TSMS	89.86	80.25	72.19	78.12	69.67	83.64
SBCIS	93.68	94.30	88.00	86.84	77.52	82.86

5. CONCLUSION AND FUTURE WORKS

We have presented an efficient model for the simultaneous bias correction and image segmentation by modeling the image as a product of true image intensities and a smooth bias field. We applied the L_0 gradient minimization to enforce the true intensities to be piecewise constant. In addition, a neighbor term was introduced to compel the piecewise constant intensities towards homogeneity. Numerical applications indicate that our method is able to capture bias of quite general profiles and can be used for images of various modalities. However, the objective functional in our work is non-convex due to the L_0 minimization, which may make the solution trapped into a local minima. Therefore, one possible future work is to extend the idea to convex variants of the Mumford-Shah model.

6. REFERENCES

[1] David Mumford and Jayant Shah, "Optimal approximations by piecewise smooth functions and associated variational problems," *Communications on pure and applied mathematics*, vol. 42, no. 5, pp. 577–685, 1989.

[2] Xiaohao Cai, Raymond Chan, and Tieyong Zeng, "A two-stage image segmentation method using a convex variant of the mumford–shah model and thresholding," *SIAM Journal on Imaging Sciences*, vol. 6, no. 1, pp. 368–390, 2013.

[3] Tom Goldstein and Stanley Osher, "The split bregman method for l1-regularized problems," *SIAM Journal on Imaging Sciences*, vol. 2, no. 2, pp. 323–343, 2009.

[4] Antonin Chambolle, "An algorithm for total variation minimization and applications," *Journal of Mathematical imaging and vision*, vol. 20, no. 1-2, pp. 89–97, 2004.

[5] James C Bezdek, LO Hall, and L_P Clarke, "Review of mr image segmentation techniques using pattern recognition," *Medical physics*, vol. 20, pp. 1033, 1993.

[6] Uros Vovk, Franjo Pernus, and Bostjan Likar, "A review of methods for correction of intensity inhomogeneity in mri," *IEEE Transactions on Medical Imaging*, vol. 26, no. 3, pp. 405–421, 2007.

[7] Mohamed N Ahmed, Sameh M Yamany, Nevin Mohamed, Aly A Farag, and Thomas Moriarty, "A modified fuzzy c-means algorithm for bias field estimation and segmentation of mri data," *IEEE Transactions on Medical Imaging*, vol. 21, no. 3, pp. 193–199, 2002.

[8] Chunming Li, Chris Gatenby, Li Wang, and John C Gore, "A robust parametric method for bias field estimation and segmentation of mr images," in *IEEE Conference on Computer Vision and Pattern Recognition*. IEEE, 2009, pp. 218–223.

[9] Chunming Li, Chenyang Xu, Adam W Anderson, and John C Gore, "Mri tissue classification and bias field estimation based on coherent local intensity clustering: A unified energy minimization framework," in *Information Processing in Medical Imaging*. Springer, 2009, pp. 288–299.

[10] Fang Li, Michael K Ng, and Chunming Li, "Variational fuzzy mumford-shah model for image segmentation," *SIAM Journal on Applied Mathematics*, vol. 70, no. 7, pp. 2750–2770, 2010.

[11] Da Chen, Mingqiang Yang, and Laurent D Cohen, "Global minimum for a variant mumford–shah model with application to medical image segmentation," *Computer Methods in Biomechanics and Biomedical Engineering: Imaging & Visualization*, vol. 1, no. 1, pp. 48–60, 2013.

[12] Li Xu, Cewu Lu, Yi Xu, and Jiaya Jia, "Image smoothing via L_0 gradient minimization," *ACM Transactions on Graphics (TOG)*, vol. 30, no. 6, pp. 174, 2011.

[13] Chunming Li, Chiu-Yen Kao, John C Gore, and Zhaohua Ding, "Implicit active contours driven by local binary fitting energy," in *IEEE Conference on Computer Vision and Pattern Recognition*. IEEE, 2007, pp. 1–7.